Formation of bubbles from a single nucleation site

JANUSZ T. CIELISKI[a*]
JACEK POLEWSKI[b]
JANUSZ A. SZYMCZYK[c]

[a] *Gdask University of Technology, Narutowicza11/12, 80-952 Gdask, Poland*

[b] *Klüber Lubrication Polska*

[c] *FH Stralsund/Univerisity of Applied Sciences, Germany*

Abstract   A systematic study on nucleate pool boiling from single artificial nucleation site to saturated, distilled water and methanol under atmospheric pressure is reported. Electrically heated sections have been employed to produce vapour bubbles. The cavities were drilled on a flat end of the copper rod. The diameter of the cavities was 0.25 mm, 0.60 mm and 1.0 mm, and the depth was approximately 0.40 mm and 0.90 mm, and 1.6 mm, respectively. Laser-photodiode system coupled with a digital oscilloscope or a PC-audio card has been utilised for measurement of release frequency. An exposure technique for measurement of bubble size has been developed. The images of the bubbles were recorded with a CCD video camera and analysed using a commercial software.

Keywords: Pool boiling; Single cavity; Frequency; Diameter

1   Background

Numerous studies of nucleate boiling heat transfer have been reported in the literature. The results of these studies have generally been given in the form of correlations. The earliest correlation for nucleate boiling is that of Rohsenow [1]. This correlation, though not based on sound reasoning

---

*Corresponding author. E-mail address: jcieslin@pg.gda.pl

of the physical mechanisms, has been very successful in predicting the observed nucleate boiling data till now [2]. However, the usefulness of such correlations diminishes very rapidly as parameters of interest start to fall outside the range of physical parameters for which the correlations were developed. Thus, some so called "mechanistic models" have been proposed in the literature [3-7]. According to [8], apart from a detailed description of the modes of heat transfer, a mechanistic model also requires, among others, a prescription of vapour bubble size and bubble release frequency. A successful prediction of the nucleate boiling heat flux requires a precise evaluation of these two key parameters. Validity of such theoretical predictions, however, is limited, mainly due to in sufficient availability of data on diameter and frequency. Due to a well-known statistical scatter of bubble nucleation and formation, further experiments are needed. Beyond that, there are contradictory statements about the effect of geometry of the nucleation site as well as pressure and heat flux density on both the frequency and the departure diameter.

A bubble generally develops from a small gas or vapour-filled cavity (artificial or natural) on the heating surface. A number of investigators have tried to produce artificial nucleation sites in order to create bubbles on definite points on the heating surface. The test sites in [9,10] consist of an air-filled glass capillary, which served quite well as a nucleation site. Others tried to make artificial cavities of definite sizes by pricking the surface with conical ground diamond needles [11-13], employing an acid technique [14] or electron-beam disintegration [15]. However, the most popular technique is drilling of cylindrical cavities [15-17], which served quite well as a nucleation site, but obviously have much larger diameters than natural cavities. In [12] and [18] cavities of reentrant or reservoir type have been investigated. The difficulty here is that a nucleus of at least critical size remains in the cavity and is instantaneously reactivated when the previous bubble detaches. These cavities allow no waiting period, a fact that has yet to be noticed in natural cavities. In present study cylindrical drilled cavities were investigated.

Many equations have been developed for the relation $fD^\alpha = const$, with the exponent α varying between -3 and $+3$ and with the constant being substituted by a combination of liquid and vapour properties, system pressure, and temperature difference. The relation between f and D – departure frequency and bubble diameter, respectively, and w – rise velocity, can be presented in the dimensional form. Some of the relations between

f, D and w are described in [19].

High-speed photography has been applied [20-22] in many laboratory experiments. But, this is very time consuming and, according to [23], not a fully reliable technique because of different bubble release and frame sequence frequency. Frequency data were taken by a stroboscope method [24]. However, own investigations [25] as well as other authors [26] have shown that this method can not be used for very high or irregular bubble generation cases. Additionally, as stated in [27], instead of "true bubble frequency" a halved one can be recorded. Mori et al. [28] have developed a new method of measurement of the rise velocity and the shape of a bubble with an electrical triple probe. More recently novel video techniques have been applied, e.g. Bergez [29] has obtained simultaneous recordings of bubble emission and wall temperature measured with thermochromic liquid crystal by use of high-speed colour video camera together with xenon flash, Tassin and Nikitopoulos [30] and Dias et al. [31] have developed a video-imaging method applied for a measurement of constant bubbling frequency based on stroboscopic video technique. Kulenovic et al. [32] have evaluated high speed video sequences by digital image processing. In recent years several laser techniques have been developed for simultaneous measurements of bubble velocity and size. Among the latter are holography [33], the Doppler method [34-36], and others [37]. Progress in electronic equipment development and laser miniaturization allows design rather inexpensive and simultaneously very reliable systems for bubbling investigation. In present study laser-photodiode system coupled with a digital oscilloscope or an PC-standard audio card has been utilised for measurement of release frequency.

The present paper is focussed on a study of the nature of vapour formation – the influence of different parameters on the release frequency and departure diameter, and particularly is devoted to:

- obtain additional experimental data under controlled conditions (heat flux density and wall superheat) for well defined nucleation site geometry (diameter and depth) and two boiling liquids (distilled water and methanol),

- development of the measurement and visualization techniques.

2 Experimental

2.1 Experimental rig

The pool boiling equipment used in this study is shown in Fig. 1. The test section was mounted in a vessel made of glass. Insulation was provided on the top, bottom and sides of the vessel. In order to keep the liquid (distilled water and methanol) in the tank at saturation temperature the electrical, auxiliary heater was installed between vessel and insulation. Two inspection windows, at the perpendicular side-walls of the vessel were furnished for visual observations. The liquid temperature was controlled by a power supplied to the auxiliary heater and measured with thermocouple. The water level in the tank was maintained at about 120 mm above the heating surface. In order to suppress undesirable vibrations the test rig was placed on a damping mass, which was additionally located on air springs.
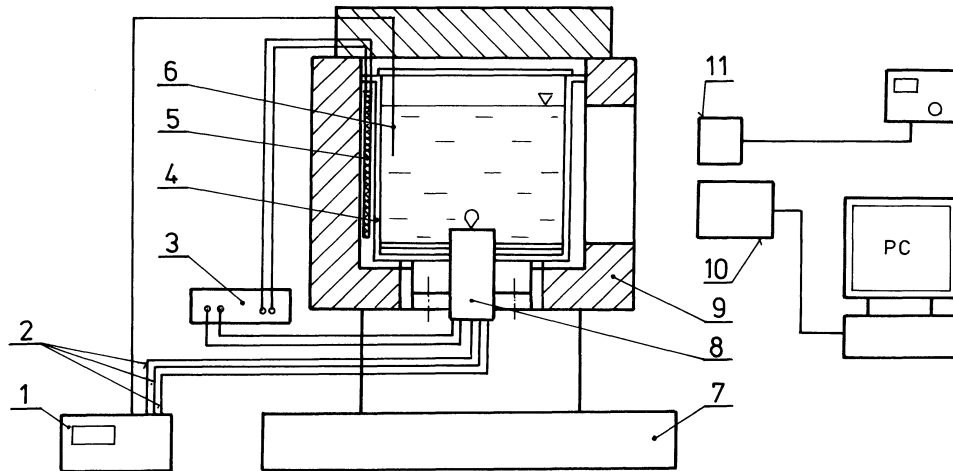

Figure 1. Schematic of the experimental rig (not to scale): 1 – logger Almemo 3290-8, 2 – thermocouples, 3 – power supply, 4 – experimental vessel, 5 – auxiliary heater, 6 – thermocouple, 7 – damping mass, 8 – test section, 9 – insulation, 10 – camera, 11 – stroboscopic.

2.2 Test section

The test section with cylindrical cavity was made of a copper rod 8 mm in diameter soft welded with a stainless steel cap 0.5 mm thick. The details

of the test section are presented in Fig. 2. The cavities were drilled on the flat end of the rod. The flat surface of the cap was polished with the water emery paper 4000. In order to avoid edge effect all edges of the cap were rounded. The rod was furnished with an electrical heater. The winding was formed of insulated high-resistance wire. The heater was supplied by means of the direct current at a controlled power rate of up to 7 W. The heating section was mounted in the bottom of the experimental vessel. The heat flux density and the temperature of the heating surface were determined using three thermocoax chromel-alumel thermocouples with a stainless steel sheath of 0.25 mm in diameter. The distances between the axis of the thermocouple wells – Fig. 3, were $\delta_1 = \delta_2 = 5$ mm and $\delta_3 = 7.5$ mm. The heat flux density was calculated using Fourier conduction equation with the thermal conductivity of the test material (electrolytic copper) for two thermocouple positions δ_1 and δ_2 with corresponding temperature differences ΔT_1 and ΔT_2 – Fig. 3. The mean heat flux density was calculated as an arithmetic mean. The simultaneous readings from these thermocouples were extrapolated to give the surface temperature with good approximation.
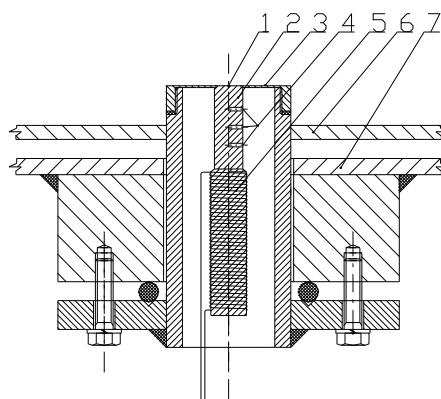

Figure 2. Details of the test section: 1 – nucleation site, 2 – conductor section, 3 – stainless steel cap, 4 – thermocouple wells, 5 – electrical heater, 6 – plate (plexiglass), 7 – bottom of the vessel.

2.3 Cavity

The diameter of the cavities (Fig. 4) was 0.25 mm, 0.60 mm, and 1.0 mm and the depth was approximately 0.4 mm, 0.90 mm, and 1.6 mm, respec-

tively. The cavities were tested without additional technological treatments after drilling and thorough cleaning by alcohol jet.
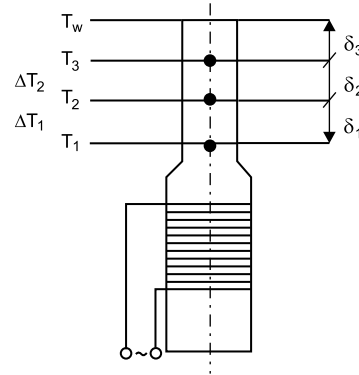

Figure 3. Symbols used in gradient method.

a)   b)   c)
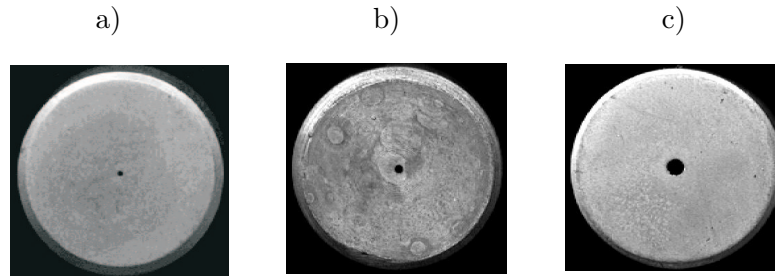

Figure 4. View of the cavities: a) 0.25 mm, b) 0.60 mm, c) 1.0 mm.

2.4   Release frequency and diameter measurement system

Laser-photodetector system coupled with a digital oscilloscope Hewlett-Packard HP 54616B (sampling rate 2 G/s) and PC-standard audio card has been utilised for measurement of release frequency – Fig. 5. The Spindler & Hoyer diode laser (type DS670) of 1 mW output power and wave length of red light 670 nm served as a light source. Spindler & Hoyer silicon photodiode E10V was utilised as a photodetector. As a rule, the detachment frequency was taken as an arithmetic mean from more than 100 peaks – bubble formation cycles, from 2 or 3 runs for a given heat flux density.
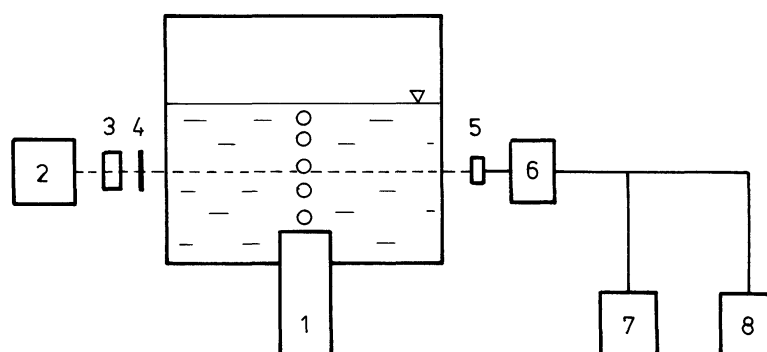
Figure 5. Schematic of the release frequency measurement system (not to scale): 1 – test section, 2 – diode laser, 3 – lens, 4 – diaphragm, 5 – photodiode, 6 – amplifier, 7 – digital oscilloscope, 8– AD-converter (PC).

Bubble diameter was estimated from the photographs taken with a high resolution (1024×1024 pixels) PIV CAM 10-30 cross correlation camera using calibration image. The equivalent diameter of bubble is defined by the following relation from the estimated bubble volume under assumption that the bubble is spherical $D = (6V/\pi)^{1/3}$. The step by step calculation procedure was described in [19]. Using the diameter of the cap as a calibration object and knowing the respective length in pixels the maximum error in single bubble diameter was estimated to fall below $\pm1\%$. The equivalent bubble diameter was checked with the formula $D_A^* = (D_1^2{\cdot}D_2)^{1/3}$, where D_1 and D_2 are the maximum horizontal and vertical diameters of the bubble. The maximum difference in equivalent bubble diameter estimation using both methods did not exceed $\pm5\%$. In the present paper "bubble volume" approach is consequently used.

As an example Fig. 6 shows the detachment of a vapour bubble from a drilled cavity 0.6 mm in diameter.

2.5   Experimental procedure

Before embarking on the main experiment, each of the test section was maintained in a pool at the temperature of 80-90^{0}C for water and 55-60^{0}C for methanol, for minimum 5 hours, in order to "age" the heating surface. Experiments were conducted at saturated, steady states under atmospheric pressure. The recorded pool temperature was 99.9$\pm$0.1^{0}C and 64.0$\pm$0.1^{0}C for water and methanol, respectively. Generally the measurements were
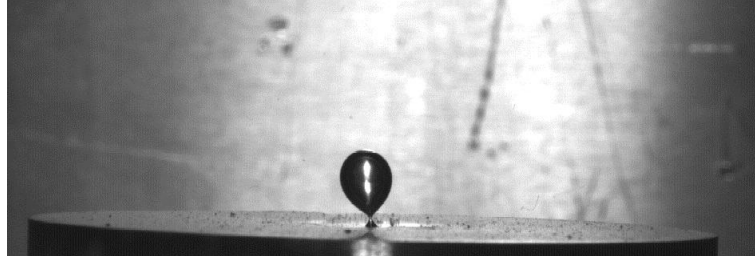
Figure 6. Detachment of vapour bubble; $D = 0.281$ cm, cavity 0.6 mm, $q = 6$ W/cm^2, $\Delta T = 6.6$ K.

conducted with increasing heat flux density, except runs of release frequency hysteresis investigation. The maximum error in heat flux density was estimated to be about $\pm15\%$ and in wall superheat $\pm10\%$.

3   Results and discussion

The notation to the present individual data points – used consequently in the presentation of the results, is given in Tab. 1.

Figure 7 displays the mean release frequency versus heat flux density. The notation to the individual data curves or points is given in Tab. 2. The known tendency of frequency increase with increase of heat flux density has been observed in the case of both tested liquids – water and methanol. As a rule, for the same heat flux density the mean release frequency recorded is even over two orders of magnitude higher for methanol than for water. In the case of water and lower heat flux density a good qualitative consistency with data by Hahne [38] has been obtained – present data are shifted to higher heat flux density, and for higher heat flux density present data are in quantitative agreement with data by [39-43]. An error in the heat flux density estimation is the possible explanation of the difference between present data and that due to Hahne et al. [38], although in both cases heat flux density was calculated from the gradient method. Nevertheless, there is no information in [38] about heat losses. In present study heat losses from the heating section – conduction through the stainless steel cap as well as natural convection from the cap, were neglected. In the case of methanol a reasonable agreement with data by Tolubinsky and Ostrovsky [39] has been recorded, particularly with cavity of 0.60 mm in diameter, although

Table 1

The notation to the present data points

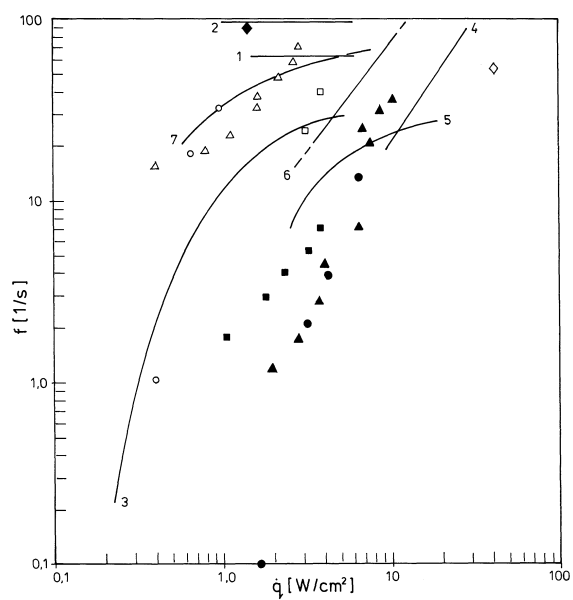| cavity	liquid	symbol
0.25 mm×0.4 mm	water	●
0.60 mm×0.9 mm	water	▲
1.0 mm×1.6 mm	water	■
0.25 mm×0.4 mm	methanol	○
0.60 mm×0.9 mm	methanol	△
1.0 mm×1.6 mm	methanol	□

Figure 7. Release frequency of vapour bubbles versus heat flux density.

Table 2

The notation to data points and curves in Fig. 7

author	cavity	liquid	surface	symbol
present results	drilled	water	copper	●, ▲, ■
present results	drilled	methanol	copper	○, △, □
Tolubinsky, Ostrovsky [39]	natural	water	permalloy, brass, copper	curve no. 1
Tolubinsky, Ostrovsky [39]	natural	methanol (96.5%)	permalloy, brass, copper	curve no. 2
Hahne et al. [38]	drilled, etched	water	stainless steel	curve no. 3
Körner, Photiadis [40]	artificial	water	nickel	curve no. 4
Hsu, Schmidt [41]	natural	water	stainless steel, aluminum	curve no. 5
Steinbrecht [42]	natural	water	brass, iron	curve no. 6, ♦ – iron
König [43]	artificial	water	copper, brass	curve no. 7
Stephan, Körner [23]	natural	methanol	silver	◇

nucleation sites in [39] were not artificial. The single point by Stephan and Körner [23] – see the notation to data points in Tab. 1, representing the mean release frequency for many natural cavities is in quantitative agreement with present data, but is shifted towards much higher heat flux density. It seems, that proper estimation of heat flux density could explain the scatter of experimental data, particularly in the case of low heat flux densities (below 1 W/cm^2). However, the dependence of release frequency versus wall superheat as a real driving force in boiling process seems to be a correct way to illustrate data.

As it is seen in Fig. 8 – the key to the individual data curves or points is given in Tab. 3, present data for water agree much better with data by Hahne et al. [38] than in Fig. 7. Additionally, excellent agreement has been recorded with data published by v. Ceumern [44] for both boiling liquids at wall superheats above 9 K. The unique theoretical model recommended in the literature for predicting the frequency of bubble departure in nucleate boiling considering the effect of surface superheat and cavity

Table 3

The notation to data points and curves in Fig. 8

| author	cavity	liquid	surface	symbol
present results	drilled	water	copper	●, ▲,■
present results	drilled	methanol	copper	○, △,□
v. Ceumern [44]	natural	water	nickel	curve no. 1
Hahne et al [38]	drilled, etched	water	stainless steel	curve no. 2
Han, Griffith [4]	natural	water	gold	♦
Singh et al. [26]	drilled by laser	water	copper	curve no. 3
Singh et al. [26]	$R = 25.4 \cdot 10^{-4}$ mm	methanol	prediction	curve no. 4
Singh et al. [26]	$R = 25.4 \cdot 10^{-3}$ mm	water	prediction	curve no. 5
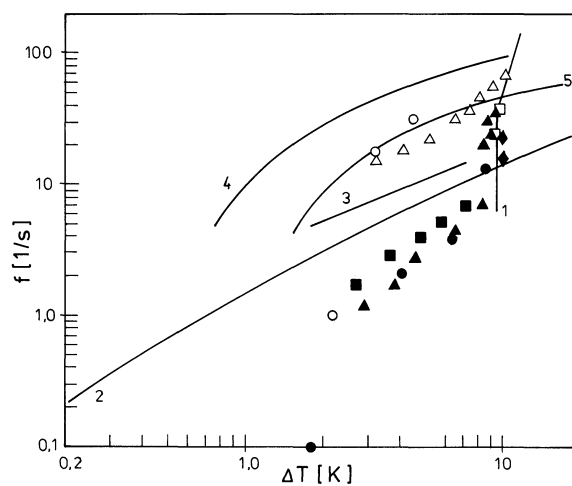
Figure 8. Release frequency of vapour bubbles versus wall superheat.

size (both radius – R in Tab. 3, and depth) is that by Singh et al. [26].
Unfortunately values predicted (for selected cavity radius presented in [26])
are overestimated, both for water and methanol. According to the model
an increase in cavity size causes a decrease in frequency. Present data for
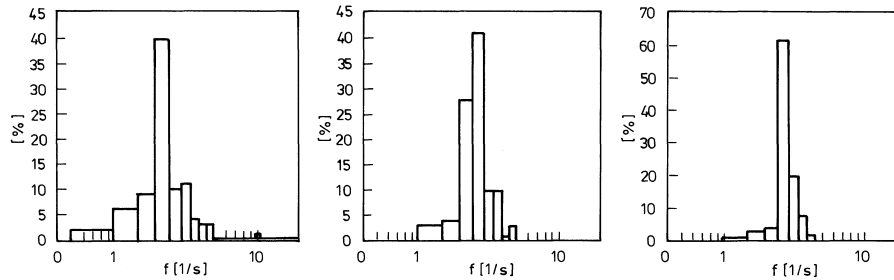methanol confirm this tendency, contrary to data recorded for water.

Figure 9. Histogram of the size distribution of bubble frequency; cavity 0.6 mm, $q =$
         3.7 W/cm^2.

Since the waiting period as well as the time of bubble formation are
subjected to stochastic fluctuations, as an example, the size distribution of
bubble frequency for cavity 0.6 mm, and three runs – for the same heat flux
density, are shown in Fig. 9. The distribution is presented as a histogram
with a logarithmic scale of frequency. One hundred formation cycles were
evaluated for each run presented in Fig. 9. The dominating frequency for
all three runs was about 2.8 Hz.

Figure 10 shows the mean release frequency versus increasing and de-
creasing heat flux density for cavity of 0.6 mm in diameter. Only very slight
hysteresis has been observed within nucleate boiling region investigated.

Figure 11 presents detachment diameter of the vapour bubbles versus
wall superheat. The horizontal lines – curves no. 6 and no. 7 in Fig. 11,
represent the predictions made with the Fritz equation [45]

$$D_A = C\beta\sqrt{\frac{2\sigma}{g(\rho_l - \rho_g)}} \tag{1}$$

with $C = 0.851$ and contact angle $\beta = \pi/4$. Except the present data for
water obtained with cavity 0.25 mm that lie direct on the curve predicted,
the other results both for water and methanol are placed above the predic-
tions. It is seen in Fig. 11 that the increase in cavity size causes increase
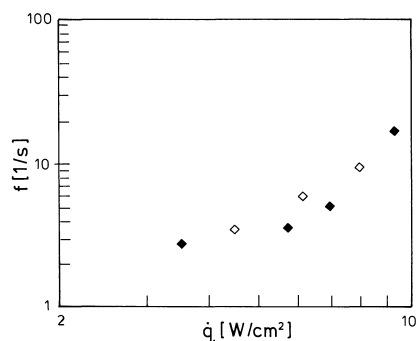
Figure 10. Release frequency hysteresis; cavity 0.6 mm; ♦ – $q(\uparrow)$, ◇ – $q(\downarrow)$.

in the bubble departure diameter. For wall superheat ca. 10 K, a good qualitative agreement with data by v. Ceumern [44] has been obtained. It is of great interest, that all quoted data – except data by Kosky [10] obtained with quite sophisticated geometry, display a change of slope – much steeper, in the vicinity of wall superheat of about 10K. The semi-empirical Fritz equation does not include the wall superheat as a parameter what can lead to big errors in bubble departure diameter predictions for wall superheats higher than 8 K.

Generally, according to present data, the bubble departure diameter of boiling methanol for given cavity size and the same wall superheat – Fig. 11, is much smaller than for boiling water. It can be attributed to the lower surface tension of methanol and as a consequence smaller surface tension force, which balances the lift forces (buoyancy, pressure force).

Figure 12 shows mean detachment frequency versus detachment diameter D. In the aim of comparison the results of other authors are displayed in Fig. 12 – the key to the individual data points or curves is given in Tab. 4. The quantities f and D are dependent variables in all experiments shown. The present results of vapour detachment frequencies from artificial nucleation sites are in reasonable agreement with the majority of quoted data, particularly for very low heat flux density (below 1 W/cm^2) such as presented in [38] and [44]. V. Ceumern [52] has differentiated two ranges of the frequency of bubbles in water versus departure diameter. In range 1, frequency $f > 20$ Hz, the departure diameter decreases with increasing frequency. In range 2, with a frequency $f < 20$ Hz, there is no change in the departure diameter by increasing wall superheat. The same tendency – for low heat flux density, was observed by Hahne et al. [38] and Cieliski and
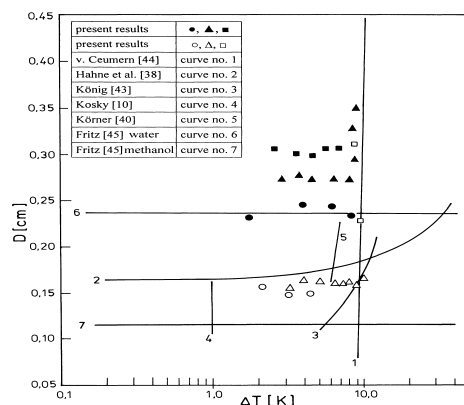
Figure 11. Detachment diameter versus wall superheat.

Szymczyk for a quite different nucleation geometry, i.e. for pin fins [51]. In the case of the present data, independently on boiling liquid or cavity size no change in the departure diameter has been recorded within the whole range of heat flux or wall superheat investigated: $0.4 \div 10.3$ W/cm^2 and $1.8 \div 10.2$ K, respectively, although, for selected cavities the detachment frequency increases as much as two orders of magnitude with the increase of wall superheat (Fig. 12).

As an example Fig. 10 shows the detachment of a vapour bubble from a drilled cavity 0.6 mm in diameter.

4   Conclusions

Detachment frequency and diameter were measured for vapour bubbles generated from single drilled cavity of different size for saturated nucleate pool boiling of water and methanol. The known tendency of frequency increase with increase of heat flux density has been observed. The results

Table 4

The notation to data points and curves in Fig. 12

| author	cavity	liquid	surface	symbol
present results	drilled	water	copper	●, ▲, ■
present results	drilled	methanol	copper	○, △, □
v. Ceumern [44]	natural	water	nickel	curve no. 1 and x
Cole [46]	natural	water	zircomium	curve no. 2
Siegel, Keshok [47]	natural	water	nickel	curve no. 3
Hatton, hall [14]	etched	water	chrome	curve no. 4
Wong et al. [6] in [44]	–	nitrogen	–	curve no. 5
Cole [48] [26]	–	azeton	–	curve no. 6
Isshiki, Tamaki [21] in [44]	–	water	–	curve no. 7
Perkins, Westwater [49]	natural	methanol	copper	curve no. 8
Staniszewski [50]	natural	methanol	copper	curve no. 9
Hahne et al. [38]	drilled, etched	water	stainless steel	curve no. 10
Cieliski, Szymczyk [51]	pin fin geometry	water	brass, stainless steel	curve no. 11
Tolubinsky, Ostrovsky [39]	natural	methanol (96.5%)	permalloy, brass, copper	◇
Westwater [34] in [21]	–	methanol	–	▽
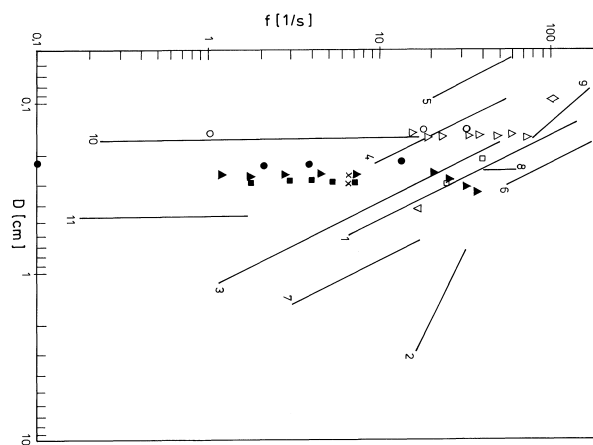
Figure 12. Release frequency of vapour bubbles versus detachment diameter.

obtained are in a reasonable agreement with published data. It is discussed
that the real driving force in boiling process is the wall superheat, so the
release frequency should be illustrated as a function of superheat rather
than heat flux density or at least has to be properly defined, for instance as
a latent heat of vaporization. It was established that for a given cavity di-
ameter the detachment bubble diameter is almost constant, whereas the de-
tachment frequency changes by two orders of magnitude. Slight frequency
hysteresis has been observed within nucleate boiling region investigated.
The model by Singh et al. [26] explains only qualitatively the observed
effect of wall superheat and cavity size on bubble departure frequency in
boiling with water and methanol. The Fritz equation [45] fails to predict
the bubble departure diameter for higher wall superheats and generally the
bubble diameter is underestimated.

Received 9 August 2002

References

[1] ROHSENOW W.M.: *A method of correlating heat transfer data for surface boiling of liquids*, Trans. ASME, **74**(1952), 969-976.

[2] PIORO I.L.: *Experimental evaluation of constants for the Rohsenow pool boiling correlation*, Int. J. Heat Mass Transfer, **42**(1999), 2003-2013.

[3] ZUBER N.: *Nucleate boiling. The region of isolated bubbles and similarity with nat-ural convection*, Int. J. Heat Mass Transfer, **6**(1963), 53-78.

[4] HAN C.Y., GRIFFITH P.: *The mechanism of heat transfer in nucleate pool boiling – Parts I and II*, Int. J. Heat Mass Transfer, **8**(1965), 887-914.

[5] JUDD R.L., HWANG K.S.: *A comprehensive model for nucleate pool boiling heat transfer including microlayer evaporation*, ASME J. Heat Transfer, **98**(1976), 623-629.

[6] HAIDER S.I., WEBB R.L.: *A transient micro-convection model of nucleate pool boiling*, Int. J. Heat Mass Transfer, **40**(1997), 3675-3688.

[7] PODOWSKI M. Z.: *Toward mechanistic multidimensional modeling of forced-convection boiling*, Proc. Boiling 2000. Phenomena & Emerging Applications, ed. A. Bar-Cohen. Alaska, **2**(2000), 531-550.

[8] LIAW S.P., DHIR V.K.: *Void fraction measurements during saturated pool boiling of water on partially wetted vertical surfaces*, ASME J. Heat Transfer, **111**(1989), 731-738.

[9] SALLALY M.: *Wärmeübertragung bei Blasenverdampfung von Flüssigkeiten an künstlichen Siedekeimen*, Chem. Eng. Sci., Vol. 21(1966), 367-380.

[10] KOSKY P. G.: *Nucleation Site Instability in Nucleate Boiling*, Int. J. Heat Mass Transfer, **11**(1968), 929-932.

[11] SERNAS V., HOOPER F. C.: *The Initial Vapour Bubble Growth on a Heat Wall during Nucleate Boiling*, Int. J. Heat Mass Transfer, **12**(1969), 1627-1639.

[12] GRIFFITH P., WALLIS J. D.: *The Role of Surface Conditions in Nucleate Boiling*, Chem. Eng. Prog. Symp. Ser., 56(30), 1960, 49-63.

[13] PRECKSHOT G. W., DENNY V.: *Explorations of Surface and Cavity Properties on the Nucleate Boiling of Carbon Tetrachloride*, Can. J. Chem. Eng., **45**(1967), 241-249.

[14] HATTON A. P., HALL I. S.: *Photographic Study of Boiling on Prepared Surface*, Int. Heat Transfer Conf. Chicago, 1966, 24-27.

[15] HOWELL J. R., SIEGEL R.: *Incipience, Growth and Detachment of Boiling Bubbles in Saturated Water from Artificial Nucleation Sites of Known Geometry and Size*, Int. Heat Transfer Conf. Chicago, 1966, 512-513.

[16] HELED Y., RICKLIS A.: *Pool Boiling from Large Arrays of Artificial Nucleation Sites*, Int. Heat Mass Transfer, **13**(1970), 503-516.

[17] HATTON A. P., JAMES D.D., LIEW T.L.: *Measurement of Bubble Characteristics for Pool Boiling from Single Cylindrical Cavities*, Int. Heat Transfer Conf. Versailles, vol. 5, B1.2, 1970.

[18] SCHIMMELPFENNIG K.: *Blasenverdampfung an Heizwandoberflächen mit künstlichen Dampfblasenkeimstellen*, Chem. Ing. Tech., **42**(1970), 16-22.

[19] SZYMCZYK J., CIELISKI J. T.: *Measurements of gas and vapour detachment frequency, diameter and rise velocity*, Trans. of the IFFM, No. 109, 2001, 69-85.

[20] MCFADDEN P., GRASSMANN P.: *The relation between bubble frequency and diameter during nucleate boiling*, Int. J. Heat Mass Transfer, **5**(1962), 169-173.

[21] IVEY H.J.: *Relationships between bubble frequency, departure diameter and rise velocity in nucleate boiling*, Int. J. Heat Mass Transfer, **10**(1967), 1023-1040.

[22] KUMADA T., SAKASHITA H., YAMAGISHI H.: *Pool boiling heat transfer-I. Measurements and semi-empirical relations of detachment frequencies of coalesced bubbles*, Int. J. Heat Mass Transfer, **38**(1995), 969-977.

[23] STEPHAN K., KÖRNER M.: *Blasenfrequenzen beim Verdampfen reiner Flüssigkeiten und binärer Flssigkeitsgemische*, Wärme-Stoffübertragung, **25**(1990), 299-304.

[24] SRINIVAS N.S., KUMAR R.: *Prediction of bubble growth rates and departure volumes in nucleate boiling at isolated sites*, Int. J. Heat Mass Transfer, **27**(1984), 1403-1409.

[25] CIELISKI J. T., SZYMCZYK J. A.: *Messungen der Frequenzen, des Durchmessers und Aufstiegsgeschwindigkeit von Gasblasen mit Hilfe einer Laser Visualisierungstechnik*, Proc. VIIth Int. Symp. on *Heat Exchange and Renewable Energy Sources*, winoujcie 1998, 85-92.

[26] SINGH A., MIKIC B. B., ROHSENOW W. M.: *Effect of superheat and cavity size on frequency of bubble departure in boiling*, ASME. J. of Heat Transfer, **99**(1977), 246-249.

[27] DAVIDSON L., AMICK E. H., JR.: *Formation of Gas Bubbles at Horizontal Orifice*, A. I. Ch. E. J., **2**(1956), No. 3, 337-342.

[28] MORI Y., HIJIKATA K., KURIYAMA L.: *Experimental study of bubble motion in mercury with and without a magnetic field*, ASME J. of Heat Transfer, **99**(1977), 404-410.

[29] BERGEZ W.: *Nucleate boiling on a thin heating plate: heat transfer and bubbling activity of nucleation sites*, Int. J. Heat Mass Transfer, **38**(1995), 1799-1811.

[30] TASSIN A.L., NIKITOPOULOS D. E.: *Non-intrusive measurements of bubble size and velocity*, Experiments in Fluids, **19**(1995), 121-132.

[31] DIAS M. I., BREIT R., RIETHMULLER M. L.: *Non-intrusive measurement technique to analyze bubble formation*, Experimental Heat Transfer, Fluid Mechanics and Thermodynamics, Brussel, 1997, 949-956.

[32] KULENOVIC R., MERTZ R., GROLL M.: *High speed flow visualization of pool boiling from enhanced evaporator tubes*, Proc. 3rd European Thermal Sciences Conf., Heidelberg, 2000, 179-185.

[33] LAUTERBORN W., HENTSCHEL L: *Cavitation bubble dynamics studied by high-speed photography and holography*, Ultrasonics, **23**(1985), 260-268.

[34] GREHAN G. ET AL.: *Measurement of bubbles by Phase Doppler technique and trajectory ambiguity*, R. J. Adrian, D. F. G. Durao, F. Durts, M. Maeda, J. Whitelow (eds), Proc. of the 7th Int. Symp. Developments in Laser Techniques and Applications to Fluid Mechanics, Lisbon, Portugal, 1994, 290-302.

[35] O'CONNOR J.P., YOU S.M., HAJI-SHEIKH A.: *Laser Doppler Anemometry measurements of bubble rise velocity and departure frequency*, Experimental Heat Transfer, **8**(1995), 145-160.

[36] RAMOS E. ET AL.: *Dynamics of boiling from a short capillary tube*, Experimental Heat Transfer, **8**(1995), 145-160.

[37] KUZMA-KICHTA YU., USTINOV A. K., USTINOV A. A.: *Investigation by laser and acoustic diagnostics method of interface oscillations during boiling*, Proc. Boiling 2000. Phenomena & Emerging Applications, ed. A. Bar-Cohen. Alaska, 2000, vol. 1, 100-115.

[38] HAHNE E., WINDISCH R., BEHREND K.: *Untersuchung von Einzelblasen an ölbeschichteten Oberflächen mit knstlichen Keimstellen*, Wärme-Stoffübertragung, **25**(1990), 299-304.

[39] TOLUBINSKY V. I., OSTROVSKY J. N.: *On the mechanism of boiling heat transfer (vapour bubbles growth rate in the process of boiling of liquids, solutions, and binary mixtures)*, Int. J. Heat Mass Transfer, **9**(1966), 1463-1470.

[40] KÖRNER W., PHOTIADIS G.: *Pool boiling heat transfer and bubble growth on surfaces with artificial cavities for bubble generation*, Heat Transfer in Boiling, eds. E. Hahne and U. Grigull, Academic Press & Hemisphere, 1977, 77-84.

[41] HSU S.T., SCHMIDT F. W.: *Measured variations in local surface temperatures in pool boiling*, ASME. J. of Heat Transfer, **83**(1961), 254-260.

[42] STEINBRECHT D.: *Beitrag zur Untersuchung der Dampfblasenbildung*, Energietechnik, Heft 5, 1969, 202-204.

[43] KÖNIG A.: *Über den Einfluss der Heizwandeigenschaften auf den Wärmeübertragung beim der Blasenverdampfung*, Diss. D83, Berlin, 1971.

[44] V. CEUMERN-LINDENSTJERNA W. CH.: *Abreibdurchmesser und Frequenzen von Dampfblasen in Wasser und wässrigen Na Cl-Lösungen beim Sieden an einer horizontalen Heizfläche*, Diss. TU Braunschweig 1975.

[45] STEPHAN K.: *Wärmeübergang beim Kondensieren und beim Sieden*, Wärme-Stoffübertragung, ed. U. Grigull, Berlin Heidelberg New York, Springer 1988.

[46] COLE R.: *A photographic study of pool boiling in the region of critical heat flux*, AIChE J., **6**(1960), 533-538.

[47] SIEGEL R., KESHOCK E. G.: *Effects of reduced gravity, on nucleate bubble dynamics in water*, AIChE J., **10**(1964), 509-516.

[48] COLE R.: *Bubble frequencies and departure volumes at subatmospheric pressures*, AIChE J., **13**(1967), 779-783.

[49] PERKINS A. S., WESTWATER J. W.: *Measurements of bubbles formed in boiling of methanol*, AIChE J., **2**(1956), 471-476.

[50] STANISZEWSKI B.: *Nucleate boiling bubble growth and departure*, Archiwum Budowy Maszyn, t. VII, 1960, 3-26.

[51] CIELISKI J. T., SZYMCZYK J. A.: *Measurements of gas and vapour bubble motion by means of visualisation techniques*, Proc. 2nd Int. Symposium on *Two-Phase Flow Modelling and Experimentation*, Pisa, Italy, 1999, ed. G. P. Celata, P. Di Marco, R.K. Shah. Pisa: Edizioni ETS**1999, vol. 3, 1441-1448.

[52] V. CEUMERN-LINDENSTJERNA W. CH.: *Bubble departure diameter and release frequencies during nucleate pool boiling of water and aqueous sodium chloride solutions*, Heat Transfer in Boiling, eds. E. Hahne and U. Grigull, Academic Press & Hemisphere, 1977, 53-75.